

The effect of spatial variations of snowpack properties on snow slope stability: A mechanically-based statistical approach

Johan Gaume^{1,*}, Jürg Schweizer¹, Alec van Herwijnen¹, Guillaume Chambon²,
Nicolas Eckert², Mohamed Naaim²

¹WSL Institute for Snow and Avalanche Research SLF, Davos, Switzerland

²IRSTEA, Grenoble, France

ABSTRACT: The spatial variability of snowpack properties has an important impact on snow slope stability and thus on avalanche formation. Hence, the determination of the link between these spatial variations and slope stability is very important, in particular for avalanche public forecasting. In this study, a statistical-mechanical model of the slab-weak layer (WL) system relying on random finite element simulation is used to investigate snowpack stability and avalanche release probability. This model accounts, in particular, for the spatial variations of WL mechanical properties and stress redistributions by elasticity of the slab. We show how avalanche release probability can be computed from release depth distributions which allow us to study the influence of WL spatial variations, slab depth and slope angle on slope stability. Finally, the importance of smoothing effects by slab's elasticity is verified and the crucial impact of spatial variation characteristics on the so-called knock-down effect on slope stability is revisited using this model.

KEYWORDS: Snow avalanche, avalanche release, slab, weak layer, spatial variability, slope stability

1 INTRODUCTION

The multiscale variation of the quantities involved in snow avalanche release and the complex microstructure of snow prevent the deterministic modelling of this phenomenon and thus the accurate prediction of snow avalanches. For instance, snowfalls and snow depths are highly variable at the regional and mountain range scales (Blanchet and Lehning, 2010; Gaume et al., 2013b). Mechanical properties of snow have also been shown to be heterogeneous at the slope scale (Kronholm and Schweizer, 2003; Kronholm et al., 2004; Schweizer et al., 2008) notably due to many process drivers such as wind and solar radiation.

Many field measurements on spatial variations of snow cover properties have been performed, in particular to address the problem of stability sampling (Jamieson and Johnston, 1993; Birkeland et al., 1995; Landry et al., 2004). Only more recently, it was recognized that the spatial variations play an important role in the fracture process leading to snow slab avalanche release (fracture initiation and crack propagation in the weak layer, Schweizer et al., 2008 and references therein). However, determining the link between snowpack spatial variability and slope stability has still not been fully

established (Bellaire and Schweizer, 2010) and is currently further investigated (Reuter and Schweizer, 2012).

To address this issue, numerical models of the slab-weak layer system have been developed taking into account the observed variations in snow properties as inputs in order to characterize their influence on avalanche release (Faillietaz et al., 2006; Fyffe and Zaiser, 2004, 2007; Gaume et al., 2012, 2013b). Interestingly, under certain conditions, these models were able to reproduce avalanche release depth and area distributions from field observations which proved to be very useful for long-term risk management.

Our aim is to use the results of Gaume et al., (2012, 2013b) concerning avalanche release depth distributions and to extend them so that the avalanche probability distribution function as a function of snowpack mechanical properties and variability parameters can be computed.

We will first present the method used to compute the avalanche probability from release depth distributions. Then, we will show how slope stability is influenced by weak-layer shear strength variability in terms of average cohesion, its standard deviation and correlation length.

2 METHODS

The mechanically-based statistical model developed by Gaume et al., 2012, 2013b enables to make finite element simulations of a slab-weak layer system taking into account the spatial variations of snowpack mechanical properties but also stress redistribution effects by elasticity of the slab. In details, the weak layer is modelled

Corresponding author address: Johan Gaume,
WSL Institute for Snow and Avalanche Research
SLF, Flüelastrasse 11, CH-7260 Davos Dorf,
Switzerland;
tel: +33 6 748 23 547;
email: gaume@slf.ch

as quasi-brittle (strain-softening) interface with a Mohr-Coulomb rupture criterion characterized by a cohesion c and a friction angle $\varphi = 30^\circ$ (van Herwijnen and Heierli, 2009). The shear strength of the weak layer is thus equal to $\tau_p = c + \sigma_n \tan \varphi$, where $\sigma_n = \rho g h \cos \theta$ is the applied normal stress. The spatial variability is accounted for through a stochastic distribution of the cohesion c with a spherical covariance function of correlation length ϵ . The average cohesion is denoted $\langle c \rangle$ and its standard deviation σ_c . The homogeneous slab is elastic with a density ρ and constant Young's modulus $E = 1\text{MPa}$ and Poisson ratio $\nu = 0.2$.

The statistical analysis of the results of this model allowed computing release depth distributions for given slope angles $\rho(h|\theta)$ which was adjusted by the following Normal distribution:

$$p(h|\theta) = \frac{1}{\sigma_h \sqrt{2\pi}} e^{-\frac{1}{2} \left(\frac{h - \langle h \rangle}{\sigma_h} \right)^2} \quad (1)$$

with $\langle h \rangle \cong \frac{\langle c \rangle}{\rho g F}$, $\sigma_h = \frac{\sigma_c f(\epsilon/\Lambda)}{\rho g F}$, $F = \sin \theta - \mu \cos \theta$, $f(\epsilon/\Lambda) = 5.45 \times 10^{-2} (\epsilon/\Lambda)^{1/3}$ a smoothing function, $\Lambda = \sqrt{E'h/k_s}$ the characteristic length of the system associated with stress redistributions due to elasticity of the slab with $E' = E/(1 - \nu^2)$ and k_s is the weak layer tangential stiffness (see Gaume et al. 2013b for more details).

From Eq. (1), assuming that Λ is almost constant (see Gaume et al. 2013b) one can define the avalanche probability P_{aval} by computing the probability that the "real" slab depth h_{real} exceeds the critical depth h coming from the mechanical stability criterion:

$$P_{\text{aval}} = P(h_{\text{real}} \geq h) = \int_0^h p(h|\theta) dh \quad (2)$$

$$\rightarrow P_{\text{aval}} = \frac{1}{2} \left[1 + \operatorname{erf} \left(\frac{\rho g h F - \langle c \rangle}{\sigma_c f(\epsilon/\Lambda) \sqrt{2}} \right) \right] \quad (3)$$

Eq. (3) is thus the expression of the avalanche probability, which can be viewed as a quantitative slope stability function which depends on the slab depth h , the slope angle θ via F and the variability parameters, namely the average cohesion $\langle c \rangle$, its standard deviation σ_c , and its correlation length ϵ . Since the erf function increases from -1 to +1 and the denominator $\sigma_c f(\epsilon/\Lambda) \sqrt{2}$ is always positive, stability significantly depends on the sign of the quantity $\rho g h F - \langle c \rangle$. Consequently, one can define two main stability cases (stable on average if $P_{\text{aval}} < 0.5$; unstable on average if $P_{\text{aval}} > 0.5$) which are represented on Figure 1.

In terms of stress and strength, one can note that analyzing the sign of $\rho g h F - \langle c \rangle$ is equivalent to analyzing the sign of $\tau - \langle \tau_p \rangle$, the difference between the shear stress due to the slab weight $\tau = \rho g h \sin \theta$ and the average shear strength of the weak layer $\langle \tau_p \rangle$.

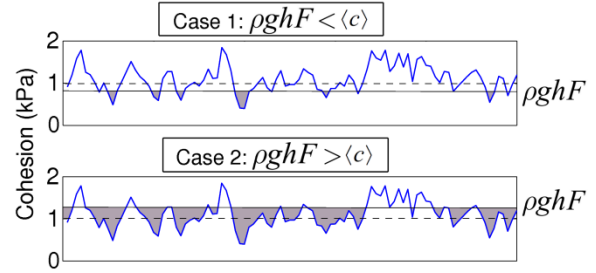


Figure 1. Diagram representing the two main stability cases depending on the sign of the quantity $\rho g h F - \langle c \rangle$. The blue curve is an example of a realization of the cohesion heterogeneity for $\langle c \rangle = 1\text{kPa}$ and $\sigma_c = 300\text{Pa}$. The zones where $\rho g h F > c$ are gray-colored. Top: stable case; bottom: unstable case.

3 RESULTS

In the following, we will show the influence of WL variability in terms of average cohesion $\langle c \rangle$, its standard deviation σ_c and its correlation length ϵ on the avalanche probability (Eq. 3).

3.1 Influence of the average cohesion

Figure 2a represents the evolution of the avalanche probability as a function of the average cohesion $\langle c \rangle$ for constant values of the cohesion standard deviation and correlation length ($\sigma_c = 300\text{Pa}$ and $\epsilon = 2\text{m}$) and for $\rho g h F = 740\text{Pa}$ corresponding to a slab density $\rho = 250\text{ kg.m}^{-3}$, a slab depth $h = 1.5\text{ m}$ and a slope angle $\theta = 40^\circ$. Note that the numerical values used in this study were arbitrarily chosen to illustrate the results.

The avalanche probability decreases from 100% to 0% with increasing average cohesion $\langle c \rangle$. The system is unstable ($P_{\text{aval}} > 50\%$) when the average cohesion is lower than $\rho g h F$ and stable ($P_{\text{aval}} < 50\%$) otherwise. From Eq. (3), one can also notice that, the smaller ϵ and σ_c are, the faster the avalanche probability decreases with $\langle c \rangle$.

3.2 Influence of the cohesion standard deviation

Figure 2b represents the evolution of the avalanche probability as a function of the cohesion standard deviation σ_c for constant values of the average cohesion and correlation length ($\langle c \rangle = 1\text{kPa}$ and $\epsilon = 5\text{m}$) and for two cases:

(i) Stable case: $\langle c \rangle > \rho g h F = 900\text{Pa}$ corresponding to a slab density $\rho = 300\text{ kg.m}^{-3}$, a slab depth $h = 1.5\text{ m}$ and a slope angle $\theta = 40.2^\circ$.

(ii) Unstable case: $\langle c \rangle < \rho g h F = 1100\text{Pa}$ corresponding to a slab density $\rho = 300\text{ kg.m}^{-3}$, a slab depth $h = 1.5\text{ m}$ and a slope angle $\theta = 42.5^\circ$. In the stable zone, for low standard deviation values ($\sigma_c < 100\text{Pa}$), the avalanche probability is equal to zero since the overall cohesion distribution is above the value of $\rho g h F$. Then, as

σ_c becomes higher than 100Pa, the avalanche probability starts to increase with σ_c and tends to 0.5. This critical standard deviation value $\sigma_c^0 = 100\text{Pa}$ corresponds to the difference between the average cohesion $\langle c \rangle$ and ρghF .

On the contrary, in the unstable zone, for $\sigma_c < \sigma_c^0$, the overall cohesion distribution is below ρghF and thus the avalanche probability is equal to 1. Then, the avalanche probability decreases with σ_c symmetrically with the stable case with respect to the $P_{\text{aval}}=0.5$ line since the absolute difference between ρghF and $\langle c \rangle$ is the same for the two cases.

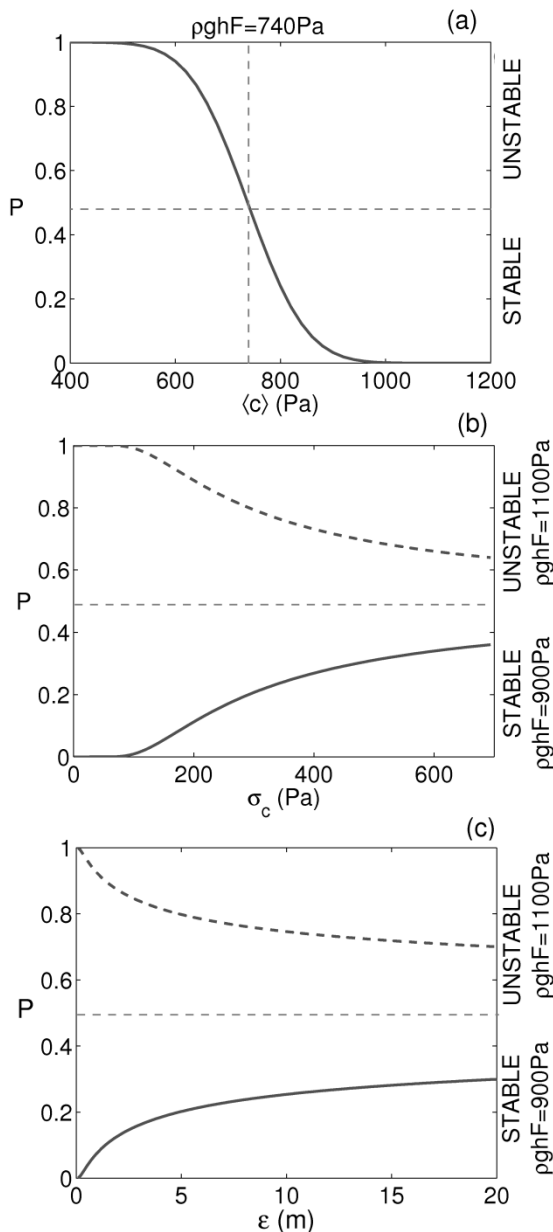


Figure 2. Evolution the avalanche probability as a function of the average cohesion $\langle c \rangle$ for $\sigma_c = 300\text{Pa}$ and $\epsilon = 2\text{m}$ (a), as a function of the cohesion standard deviation σ_c for $\langle c \rangle = 1\text{kPa}$ and $\epsilon = 5\text{m}$ (b) and as a function of the correlation length ϵ for $\langle c \rangle = 1\text{kPa}$ and $\sigma_c = 300\text{Pa}$ (c).

3.3 Influence of the cohesion correlation length

Figure 2c represents the evolution of the avalanche probability as a function of the correlation length ϵ for constant values of the average cohesion and standard deviation ($\langle c \rangle = 1\text{kPa}$ and $\sigma_c = 300\text{Pa}$) and for the two stable/unstable cases presented above. For the stable case, the avalanche probability initially increases strongly with ϵ between 0 and 2 m and then more slowly up to the limit $P_{\text{aval}}=0.5$ when $\epsilon \rightarrow \infty$.

On the contrary, in the unstable case, the avalanche probability decreases with ϵ and, as well as for the evolution with σ_c , symmetrically with the stable case with respect to the $P_{\text{aval}}=0.5$ line.

Note that the influence of the correlation length ϵ is taken into account via the smoothing function f (Eq. 1) which is always lower than 1 within the set of simulated parameters and tends to reduce the variability when ϵ is low compared to the characteristic elastic length of the system Λ which is approximately equal to 0.9m in this case. This is due to redistribution of stresses induced by the elasticity of the slab.

4 DISCUSSIONS & CONCLUSION

We presented a method based on random finite element simulations aimed at linking the characteristics of weak layer spatial variability to slope stability.

Spatial variations of weak layer mechanical properties strongly influence avalanche formation and thus slope stability (Schweizer et al., 2008). Our results show that stability mostly depends on the difference between the shear stress due to the slab τ and the average shear strength of the weak layer $\langle \tau_p \rangle$ which is a function of the average cohesion $\langle c \rangle$. However, our study also highlighted two other key factors: the spatial scale of variability (or correlation length) ϵ and the cohesion standard deviation σ_c . In the most common stable case, the average shear strength is higher than the shear stress due to the slab. As a consequence, the critical length of the initial failure a – i.e. the length of the zones for which

$$\tau - \tau_p = \rho ghF - c < 0, \quad (4)$$

represented in gray in Figure 1a – is lower than the correlation length ϵ . In this case, both the overall variation σ_c and the spatial scale of variability ϵ have a significant “knock-down” effect on slope stability and thus can promote instability. On the contrary, if $\tau - \tau_p > 0$, this critical length a is higher than the correlation length ϵ , which has in this case, as well as the standard deviation σ_c , a stabilizing effect rather preventing avalanche formation, a less intuitive result.

Finally, one should note that this study was made under the assumption that the average release depth $\langle h \rangle$ obtained from the random finite element simulations is approximately equal to $\langle c \rangle / (\rho g F)$ derived from the averaged Mohr-Coulomb criterion (Eq. 1). In fact, Gaume et al. (2013b) have shown that $\langle h \rangle$ is always slightly smaller than $\langle c \rangle / (\rho g F)$ and that the difference tends to increase with increasing correlation length ϵ . Fyffe and Zaiser (2006) have also shown that $\langle h \rangle$ decreases with the coefficient of variation $CV = \sigma_c / \langle c \rangle$. The important outcome of this remark is that by refining the presented results by taking into account the influence of ϵ and σ_c on the average slab depth $\langle h \rangle$, the “knock-down” effect might be amplified, allowing a transition from stable to unstable zones and reciprocally only by varying the correlation length ϵ and/or the cohesion standard deviation σ_c , which was not possible with the assumptions we used.

5 REFERENCES

- Bellaire, S. and J. Schweizer, 2011. Measuring spatial variations of weak layer and slab properties with regard to snow slope stability. *Cold Reg. Sci. Technol.*, **65**(2), 234–241.
- Birkeland, K., B. Hansen, and R. Brown, 1995. The spatial variability of snow resistance on potential avalanche slopes. *J. Glaciol.*, **41**(137), 183–189.
- Blanchet, J. and M. Lehning, 2010. Mapping snow depth return levels: smooth spatial modeling versus station interpolation. *Hydrol. Earth Syst. Sc. Disc.*, **7**, 6129–6177.
- Faillietaz, J, F Louchet and J.R Grasso, 2006. Cellular automaton modelling of slab avalanche triggering mechanisms : from the universal statistical behaviour to particular cases, *Proceedings of the ISSW*, 174-180.
- Fyffe, B and M Zaiser, 2004. The effects of snow variability on slab avalanche release, *Cold Reg. Sci. Technol.*, **40**, 229–242.
- Fyffe, B and M Zaiser, 2007. Interplay of basal shear fracture and slab rupture in slab avalanche release, *Cold Reg. Sci. Technol.*, **49**, 2638.
- Gaume, J., G. Chambon, N. Eckert and M. Naaim, 2012. Relative influence of mechanical and meteorological factors on avalanche release depth distributions., *Geophys. Res. Lett.*, **39**, L12401
- Jamieson, B and C Johnston, 1990. In-situ tensile tests of snowpack layers, *J. Glaciol.*, **36**(122), 102–106.
- Gaume, J., G. Chambon, N. Eckert and M. Naaim, 2013a. Influence of weak-layer heterogeneity on snow slab avalanche release: Application to the evaluation of avalanche release depths., *J. Glaciol.*, **59**(215), 423-437
- Gaume, J., N. Eckert, G. Chambon, M. Naaim, and L. Bel 2013b. Mapping extreme snowfalls in the French Alps using max-stable processes, *Water Resour. Res.*, **49**(2), 1079-1098, doi:[10.1002/wrcr.20083](https://doi.org/10.1002/wrcr.20083).
- Jamieson, B. and C. Johnston, 1993. Rutschblock precision, technique variations and limitations. *J. Glaciol.*, **39**(133), 666–674.
- Kronholm, K. and J. Schweizer, 2003. Snow stability variation on small slopes. *Cold Reg. Sci. Technol.*, **37**(3), 453–465.
- Kronholm, K., Schneebeli, M., Schweizer, J., 2004. Spatial variability of micropenetration resistance in snow layers on a small slope. *Annals of Glaciology* **38**, 202–208.
- Landry, C., K. Birkeland, K. Hansen, J. Borkowski, R. Brown, and R. Aspinall, 2004. Variations in snow strength and stability on uniform slopes. *Cold Reg. Sci. Technol.*, **39**(2-3), 205–218.
- Reuter, B. and J. Schweizer, 2012. Variations of snow depth and snowpack stability at the basin scale. *Geophys. Res. Abstr.*, **14**, EGU2012–14138.
- Schweizer, J., K. Kronholm, J. Jamieson, and K. Birkeland, 2008. Review of spatial variability of snowpack properties and its importance for avalanche formation. *Cold Reg. Sci. Technol.*, **51**(2-3), 253–272.
- van Herwijnen, A. and J. Heierli, 2009. Measurements of crack-face friction in collapsed weak snow layers. *Geophys. Res. Lett.*, **36**, L23502.